Al-Azhar University Civil Engineering Research Magazine (CERM)
Vol. (40) No. (2) April, 2018

Monitoring Effect of Geomagnetic Storm on Ionosphere Using GPS Observation

Heba Tawfeek[1], Ahmed Sedeek[2],Mostafa Rabah[3], Gamal El-Fiky[1]
1. Faculty of Engineering, Zagazig University, Egypt,
2. Higher Institute of Engineering and Technology, El-Behira, Egypt,
3. Benha Faculty of Engineering, Benha University, Egypt.

الملخص العربى
يعرف رسم الخرائط الأيونوسفيرية بأنه الأسلوب الذى يطبق قيم المحتوي الإلكتروني الكلي العمودي (VTEC) المقاسة في وقت واحد لتوليد خرائط VTEC في فترة زمنية محددة. وقد أجريت العديد من الدراسات لرسم خرائط الأيونوسفير. وفي السنوات الأخيرة، تستخدم عمليات رصد نظام تحديد المواقع على نطاق واسع لهذا الغرض. وقد درس هذا البحث خصائص الاختلاف في VTEC باستخدام نموذج صفر الاختلاف للطور فى النشاط الأيونوسفيري المسمى (ZDPID). وقد طبق هذا النموذج مفهوما لحل غموض موجات GPS باستخدام متسلسلة ضبط أقل مربع (SLS) لتثبيت موجات الغموض في عمليات رصد الطور لكل ظهور للقمر . و تم كتابة النموذج المقترح باستخدام كود ماتلاب. وقد استخدم هذا النموذج لإنتاج الخرائط الإقليمية اللحظية للأيونوسفير. ويظهر هذا البحث مفهوما وأمثلة عملية للتخطيط الفوري للغلاف الأيوني. ولهذا السبب، تم اختيار محطتين من الخدمة الدولية لتحديد المواقع (IGS) من مناطق خطوط العرض العليا وخطوط العرض المتوسطة. وقد تم إنشاء خرائط لحظية لكل من أيام هادئة وعاصفة باستخدام ZDPID. وقد تم مقارنة جودة التمثيل الأيونوسفير مع خرائط إيونوسفير العالمية (GIMs)، والتي تستخدم عادة كمرجع. واستخدمت محطتا GPS آخران في مصر لتوليد خرائط الأيونوسفير الإقليمية في هذه الأيام فوق دلتا النيل بمصر.

Abstract

Ionospheric mapping is defined as a technique applying simultaneously measured TEC values to generate VTEC maps referred to a specific time epoch. Many studies have been performed for ionosphere mapping. In recent years GPS observations are widely used for this purpose. This paper studied variation characteristics of ionospheric vertical total electron contents (VTEC) using Zero Difference Phase Ionospheric Delay model called (ZDPID). This model applied a concept for GPS phase ambiguity resolution using Sequential Least Square Adjustment (SLSA) to fix ambiguity term in phase observations was written using MATLAB code. This model was used to produce the epoch-specific instantaneous regional maps of the ionosphere. This paper demonstrates concept and practical examples of instantaneous mapping of the ionosphere. For this reason, two stations from the International GPS service (IGS) have been selected from high-latitude and mid-latitude regions. Instantaneous maps have been generated for both quiet and stormy days by using ZDPID.The quality of the ionosphere representation has been compared to IGS Global Ionosphere Maps(GIMs), which is generally used as a reference. Another two GPS stations in Egypt were used to generate regional ionosphere maps in these days over Nile Delta, Egypt.

Key words: ZDPID, Ionosphere mapping, PPP, high-latitude and mid-latitude.

1. Introduction

During the last decade GPS has become an interesting tool for ionospheric investigations. The ionosphere is a region of ionised gas that extends from 70 km ~1000 km. In that region free electron density affects the propagation of radio frequency electromagnetic waves. Spatial and temporal characteristic effects of the ionosphere on radio wave propagation, interest various study areas including space-based observation systems as well as communication systems and safety-critical systems (Liu and Gao, 2004).The ionosphere is in its nature varying over time. The main time characteristics include the 24 hour periodicity with a peak at 14.00 local time and low during night time, a yearly trend with peaks around equinoxes and a low, but longer peak during summertime, and a 11 year time period correlated with the sunspot number as described in e.g. (Misra and Enge, 2006).

The wide spread effect of the ionosphere on various areas has made ionospheric studies popular subject. Ionospheric mapping is defined as a technique applying simultaneously measured total electron content(TEC) values to generate TEC maps referred to a specific time epoch(Stanislawska et. al. 2000).With the help of large number of tracing stations, GPS observations can be used for monitoring ionospheric conditions during disturbed and quiet geomagnetic conditions. Ex: GNSS analysis centers provide GIMs(Global Ionosphere Maps) on a daily basis. Many studies have been performed for regional ionosphere mapping. (Wielgosz et. al., 2003a)and (Nohutcu et. al., 2010) and Salih Alcay et al. 2012). Regional ionospheric maps are routinely produced and made available on the Internet (Sardon et al., 1995; Jakowski et al., 1996). The characteristics of the variation of the Total Electron Content (TEC) in the ionosphere are very different from latitude to latitude and thus an important factor for obtaining an accurate model is to use data from local GNSS reference stations, as described in Hargreaves (1992). For this reason, the IGS station (METS) was chosen as a high-latitude station at approximately 60°N latitude the daily length varies considerable, compared to mid- latitudes station (SOFI), making the daily variation of the ionosphere more different over the year. By the help of these two stations, regional ionosphere maps have been generated for both quiet and stormy days by using Zero Difference Phase Ionospheric Delay (ZDPID). This model is based upon utilizing dual frequency GPS carrier phase observation because of its high precision to produce Ionospheric maps using a single GPS station (Zero Differenced) under MATLAB environment. In the present paper, Sequential Least Square Adjustment (SLSA) is considered to fix the ambiguity term to overcome the singularity in the observation equation. Due to the lack of GPS stations over the equatorial, North Africa and Atlantic in IGS network, ZDPID is suggested to be able to produce ionospheric maps over Egypt and over any other GPS station accurately. Therefore, the Ionospheric activity over Nile Delta, Egypt, was investigated using two GPS stations for both quiet and stormy days. The GPS data used here are from regional GPS reference observed by National Research Institute of Astronomy and Geophysics (NRIAG).Two-dimensional maps of absolute VTEC are derived with time resolution of 30 seconds and spatial resolution of $0.5^{\circ} \times 0.5^{\circ}$ in latitude and longitude interpolated with kiriging method.

2. Data and Methodology

2.1 ZDPID Model

For analysis of the temporal variations of the ionosphere withthe difference of carrier phase the GPS signals passes along individual satellite were used. We used in the present paper the MATLAB source code called ZDPID which introduced in. This model based on zero difference of carrier phase. Figure (2) shows Flowchart of the stages of determination of VTEC mapping. We firstly entered the observations file in RINEX format to read the observations of dual-frequency GPS receiver (L1 and L2) which consists of two codes and two carrier phase observations and station coordinates. Then, the SP3 files of this day and pervious day file and next day file were entered to make a linear interpolation for GPS satellite orbits positions from 15-min time step to 30 sec satellite positions between these points position is then transformed to a local coordinate frame, East North and Up (ENU) system. The transferred ENU was used to calculate elevation and azimuth angles(E & A)(Misra and Enge, 2001; Sunehra, 2013).The ionosphere assumed to be concentrated on a spherical shell of infinitesimal thickness located at altitude, for example, of 450 km above Earth's surface, i.e., forming single layer model (SLM) (Rocken et al., 2000).

Ionospheric Pierce Point (IPP) is the intersection point between the satellite receiver line-of-sight, and the ionosphere shell. IPP location can be computed by providing reference station coordinates (ϕ_r, λ_r) as shown in figure (1), then the geographic latitude and longitude of IPP can be computed according to elevation and azimuth angle of satellite such as follows (Dahiraj, 2013):

$$\psi = \pi / 2 - E' - E \qquad (1)$$

Where:

ψ : The offset between the IPP and the receiver;

E' and E: the elevation angles at the IPP and receiver.

$$E' = \sin^{-1}\left(\left(\frac{R_E}{R_E + H}\right)\cos E\right) \qquad (2)$$

Where:

RE: is the mean radius of the spherical Earth (6371 km)

H: is the height of IPP (it is taken to be 450 km)

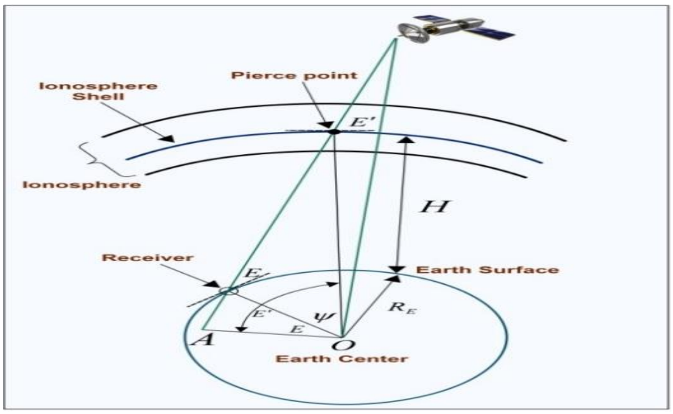

Figure (1): Elements of the spherical ionospheric shell model (Sedeek et al.,2017).

$$\varphi_{IPP} = \sin^{-1}(\sin(\varphi_r).\cos(\psi) + \cos(\varphi_r).\sin(\psi).\cos(A)) \qquad (3)$$

$$\lambda_{IPP} = \lambda_r + \frac{\psi.\sin(A)}{\cos(\varphi_{IPP})} \qquad (4)$$

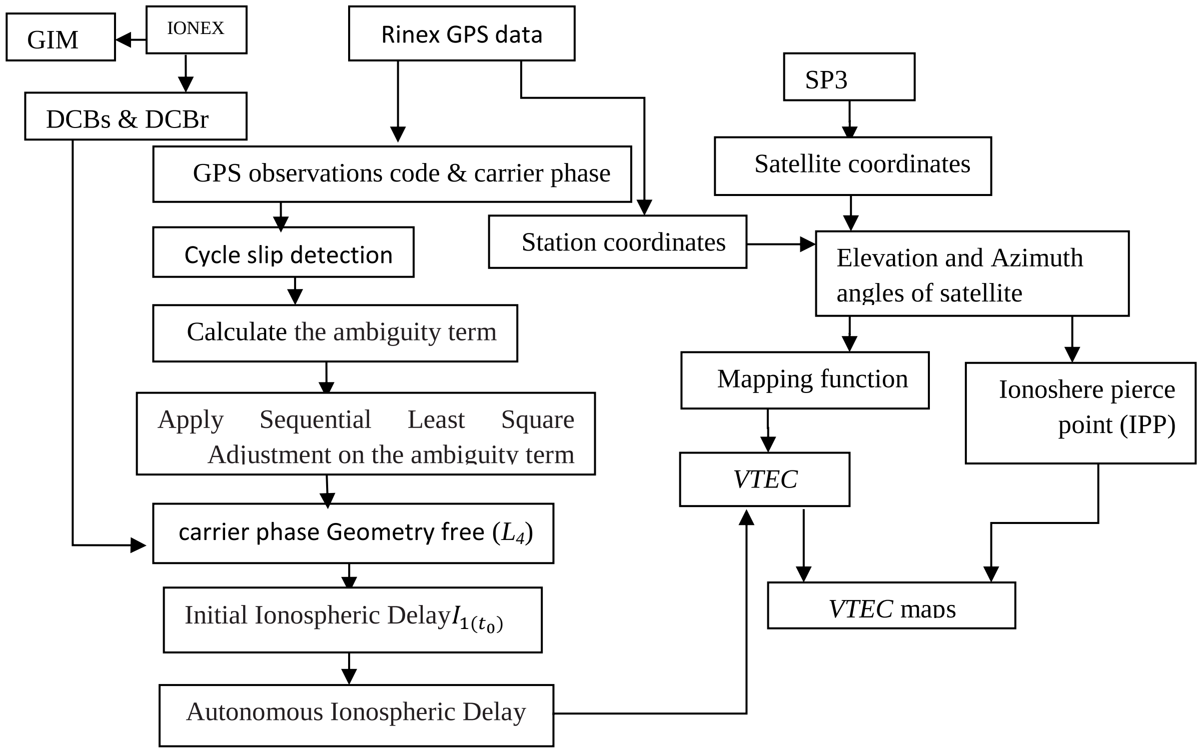

Figure (2): Flowchart of the stages of determination of VTEC.

This model used Melbourne-Wübbena (1985) Linear Combination is utilized to detect and repair cycle slips. And used Ionosphere-free and Geometry-free Combinations algorithms to estimate the ambiguity term from the observations equations as follows (Guochang Xu, 2004) :

$$\begin{bmatrix} \lambda_1 N_1 \\ \lambda_2 N_2 \\ B1 \\ \varepsilon \end{bmatrix} = \begin{bmatrix} 1-2a & -2b & 0 & 2 \\ -2a & -2a-1 & 0 & 1 \\ 1/q & -1/q & 0 & 0 \\ a & b & 0 & 0 \end{bmatrix} \begin{bmatrix} P1 \\ P2 \\ \Phi 1 \\ \Phi 2 \end{bmatrix} \qquad (5)$$

Where:

$a = f_1^2/(f_1^2 - f_2^2)$,
$b = -f_2^2/(f_1^2 - f_2^2)$,
$q = f_1^2 * (1/f_1^2 - 1/f_2^2)$.

P1 and P2 Pseudo-range measurements on L1 and L2 frequencies, respectively, in meter;

Φ1 and Φ2 carrier-phase measurements on L1 and L2 frequencies, respectively, in meter;

N1andN2 integer ambiguities on L1 and L2 frequencies, respectively, in cycles;

λ1 and λ2 carrier-phase wave length on L1 and L2 frequencies, respectively, in meters;

ε error,

B1 =I1, B1 is ionospheric parameters in the path and zenith,

f_i^2 Frequency where i: 1; 2.

This model applies Sequential Least Square Adjustment to fix the ambiguity term to be one value of all epochs of every rise of satellite. Secondly, the geometry-free linear combination of GPS observations is classically used for ionospheric investigations and it is obtained by subtracting simultaneous of carrier phase observations (Φ1-Φ2).

$$L4(t) = \Phi_{GF} = \Phi_1 - \Phi_2 = (\gamma - 1) I_1 + \lambda_1 N_1 - \lambda_2 N_2 + \text{DCBs} + \varepsilon_{(\Phi_1 - \Phi_2)} \quad (6)$$

Where: ε(Φ1 - Φ2) is the noise term in phase equation can be neglected for the sake of simplicity, the factor γ is the factor to convert the ionospheric delay from L1 to L2 frequency $\gamma = \frac{f_1^2}{f_2^2}$, DCBs is the difference carrier-phase hardware delays bias betweenL1& L2 frequency for receiver and satellite. To compute the Initial Ionospheric Delay$I_{1(t_0)}$ from epoch (t0) to (t0 + n), the fallowing equation are used:

$$L_{4(t_{0+n})} - \frac{f_1^2 - f_2^2}{f_1^2} \sum \partial I_{1(t_0, t_{0+n})} = (\lambda_1 N_1 - \lambda_2 N_2) + \frac{f_1^2 - f_2^2}{f_1^2} \left(I_{1(t_0)}\right) + \text{DCBs} \quad (7)$$

And the autonomous Ionospheric Delay:

$$I_{1(t_{0+n})} = I_{1(t_0)} + \sum \partial I_{1(t_0, t_{0+n})} \quad (8)$$

and $\partial L_{4(t_0, t_{0+k})} = L_{4(t_{0+k})} - L_{4(t_0)} = \frac{f_1^2 - f_2^2}{f_1^2} \partial I_{1(t_0, t_{0+k})}$ (9)

Where: k is epoch number (t_0<k<n) and $I_{1(t_0)}$ is the ionosphere delay at epoch (t0).

finally, the VTEC estimated at each epoch to produce the maps and its mapping function from equation (8&2).

$$VTEC = F(E) \frac{I_1 . f_1^2}{40.3}, \quad F(E) = \frac{1}{\cos(E')} \quad (10)$$

2.2 VTEC Maps Data

In the present study, the data set consisting of 24-hour data at 30 sec intervals, elevation cut off angle is 10˚. Using dual-frequency receivers which record both the differential carrier phase and the differential group delay from up to eight satellites simultaneously. This means that more than 25,000 VTEC observations/day. SOFI and METS IGS station, which are located in mid-latitude and high-latitude regions respectively, have been chosen. In order to determine the geographical location of the regional maps, 30˚ - 45˚ latitudes and 10˚ - 35˚ longitudes for SOFI and also 47.5˚ - 70˚ latitudes and10˚ - 35˚longitudes for METS have been selected. This region covers the IPPs location for most of the processed epochs. The TEC values were interpolated by Kriging method with Surfer software (V.12). The studied region was gridded with space 0.5˚ × 0.5˚ to create high-resolution instantaneous TEC maps. In the current study, the satellite and receiver DCB were taken from IGS products (IONEX files). Another two station from Egypt Nile Delta called HELW and SAID observed by NRIAG. In order to determine the geographical location of the regional maps, 20˚ - 40˚ latitudes and 20˚ - 40˚ longitudes, the satellite DCB were taken from IGS products (IONEX files)and receiver DCB estimated from (sedeek et al., 2017). To know the stormy days, there is kp index. It is a scale of numbers between 0 – 9 known as the planetary index. It is used to characterize the magnitude of geomagnetic storms. Kp is an excellent indicator of disturbances in the Earth's magnetic field and is used by SWPC to decide whether geomagnetic alerts and warnings need to be issued for users who are affected by these disturbances. Geomagnetic storms, indicated by a Kp = 5 or higher, have no direct effect on propagation. For doing this both stormy (2015, DAY105) and quiet (2015, DAY 96) days have been considered. In order to see the effect of storm on ionosphere, k_p index values for pertinent days are given in figure (3) and (4). Figure (5) showed Location of the two Delta Stations, Egypt, and IGS stations used to estimate the regional TEC values.

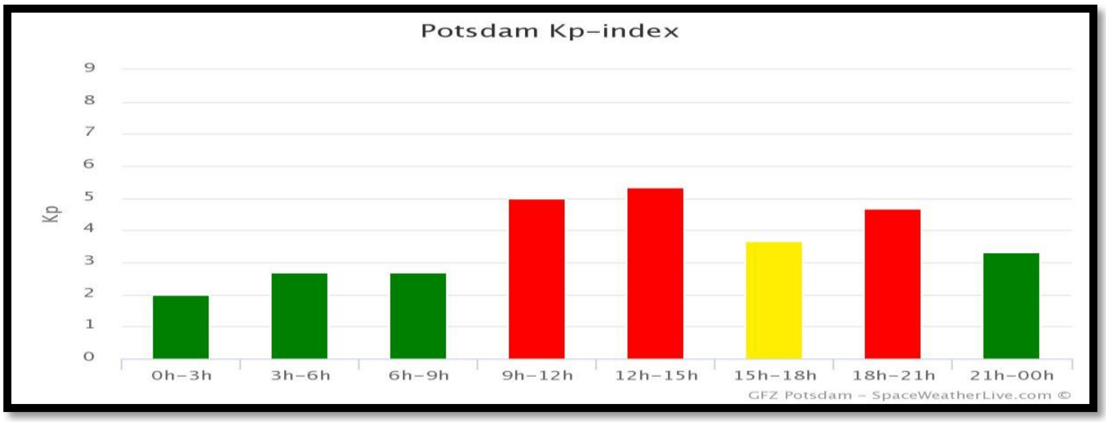

Figure (3) Kp values for 2015, DAY 105 (https://www.spaceweatherlive.com).

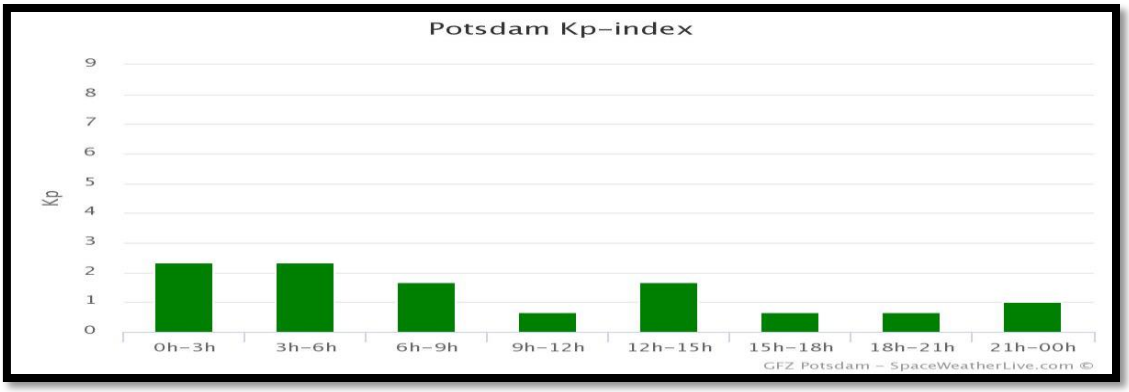

Figure (4). Kp values for 2015, DAY 96 (https://www.spaceweatherlive.com).

As it can be seen in figure (3), geomagnetic storm is extreme for 9-12, 12-15 and 18-21 time periods. However there is no storm occur for the day 96 as shown in figure (4)

3. Results and Discussions

VTEC maps cover a 24 hourly time period at intervals of 2 hours. Figure (6) and (7) illustrate the vertical TEC maps for high-latitude station, METS on day96 and 105 respectively which were produced with ZDPID technique with two-hour intervals between each map. For the comparison purpose, an area covering regional model was extracted from Global ionosphere Maps(GIM) which were downloaded from Centre for Orbit Determination in Europe (CODE)(IONEX file). We select a region located between 47.5˚~ 70˚north geographic latitude and 10˚~ 35˚ longitude. This region covers the IPPs location for most of the processed epochs. The TEC values were interpolated by Kriging method with Surfer software (V.12).We grid the studied region with space 0.5˚ × 0.5˚ to create high-resolution instantaneous TEC maps are given in figure (8) and (9) for day 96 and 105 respectively. Also comparison between GIMs and vertical TEC map for mid-latitude station, SOFI, is given in figures (10-11) and (12-13) for day 96 and 105 respectively. ZDPID was used to produce ionospheric maps over Nile Delta, Egypt. Therefore, the Ionospheric activity over Nile Delta, Egypt, was investigated using two GPS stations, HELW and SAID are given in figures (14-15) and (16-17) for day 96 and 105 respectively. A region from GIM located between geographic latitude 20˚~ 50˚ N and longitude 10˚~ 40˚ E was selected in figures (12-13)to cover the IPPs location for most of the processed epochs of SOFI and the two stations in Egypt. The TEC values were interpolated by Kriging method with Surfer software (V.12). The studied regions was gridded with space 0.5˚ × 0.5˚ to create high-resolution instantaneous TEC maps.

Figure (5) Location of the two Delta Stations, Egypt, and IGS stations used to estimate the regional *TEC* values

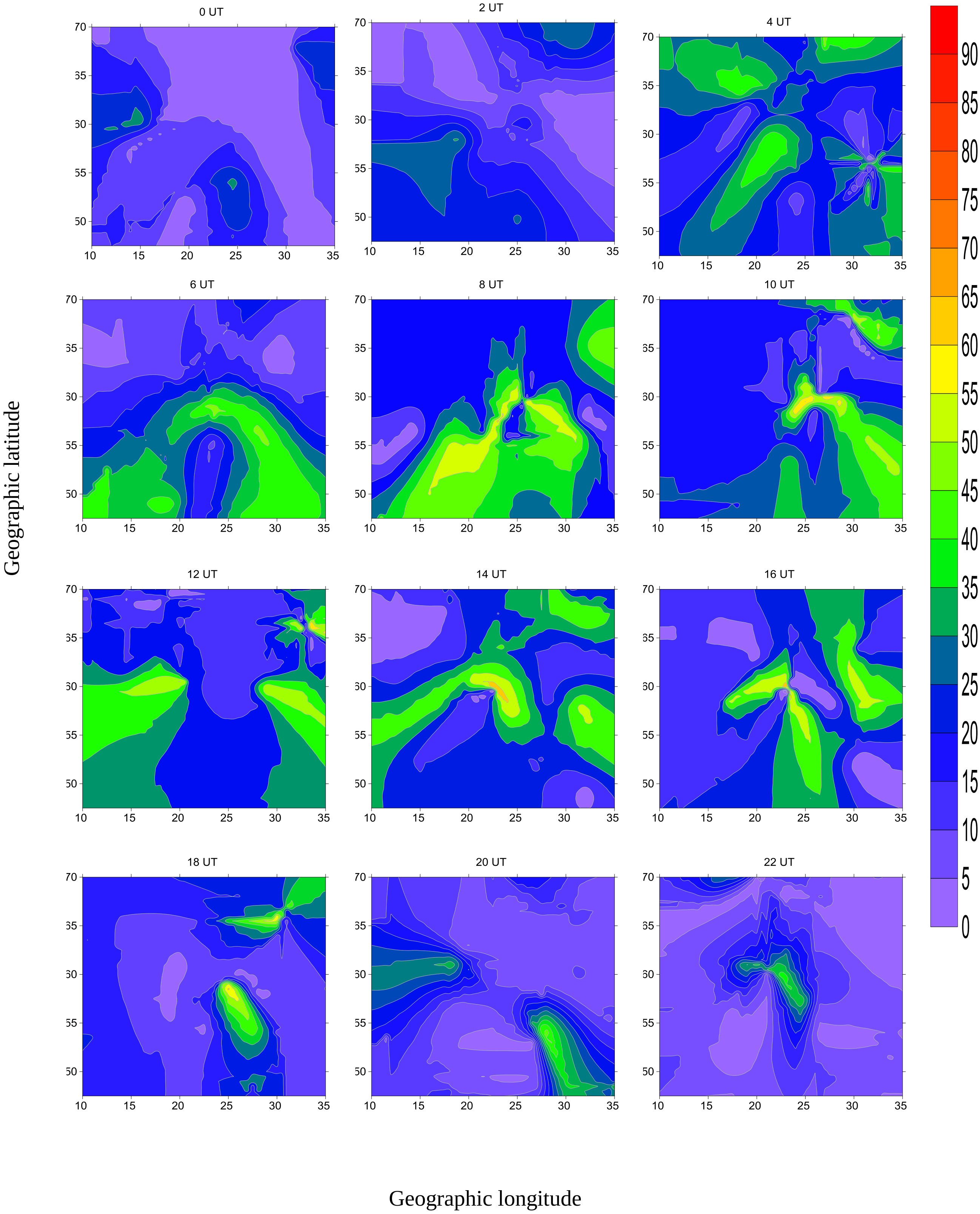

Figure (6). VTEC maps for METS station of Day 96 (2015)

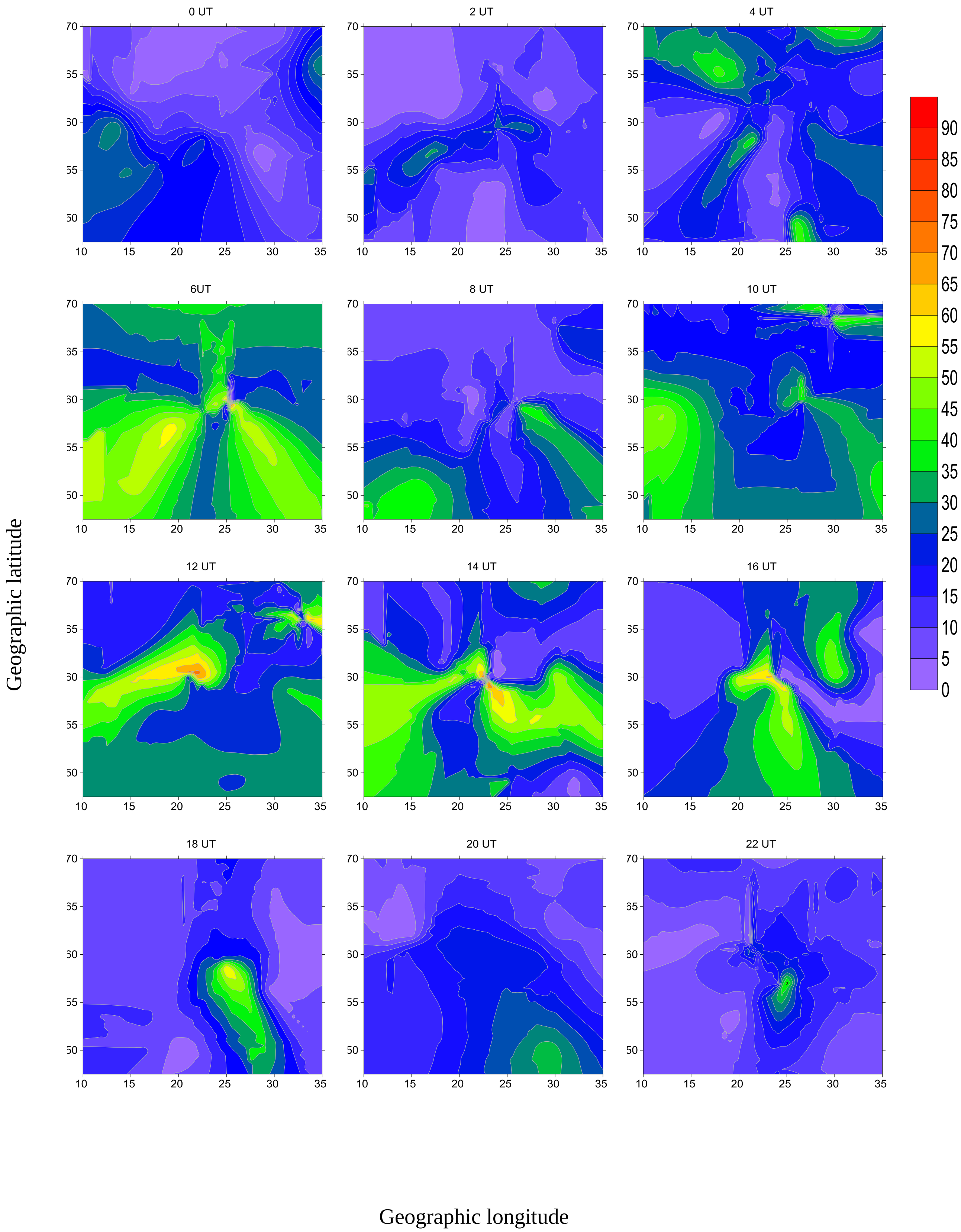

Figure (7). VTEC maps for METS station of Day 105 (2015).

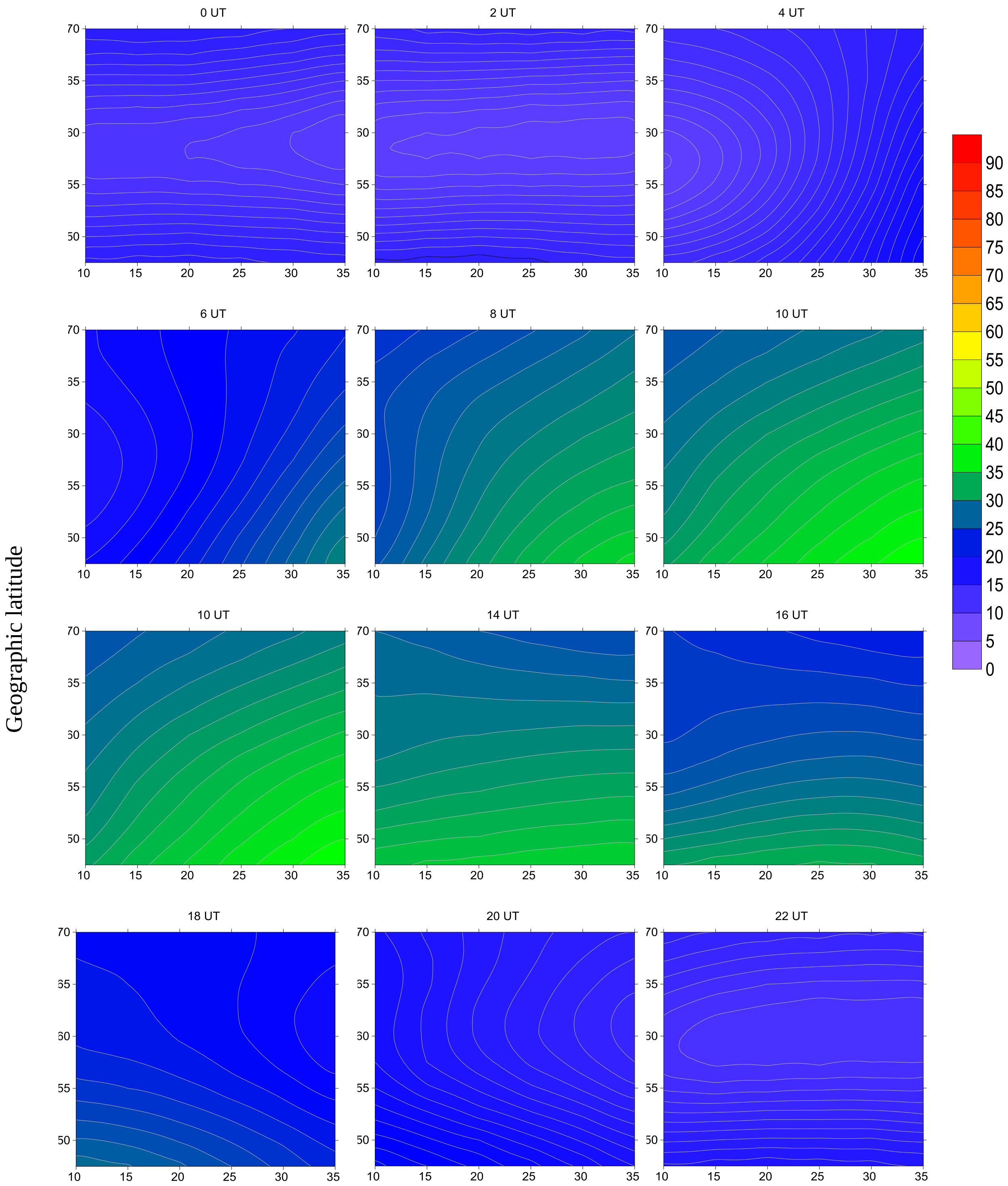

Geographic longitude

Figure (8) TEC maps from GIM, Day 96-2015.

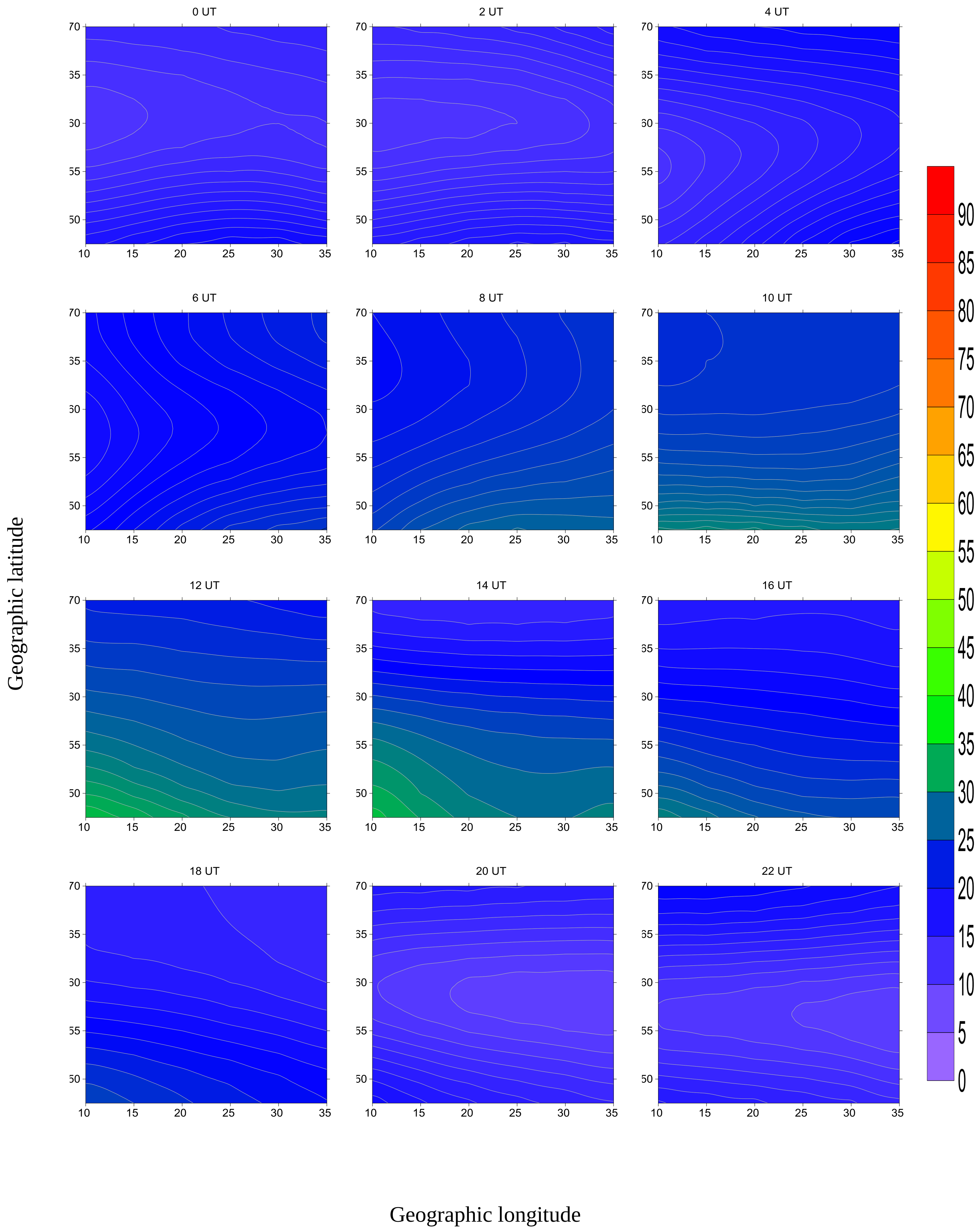

Figure (9) TEC maps from GIM, Day 105-2015.

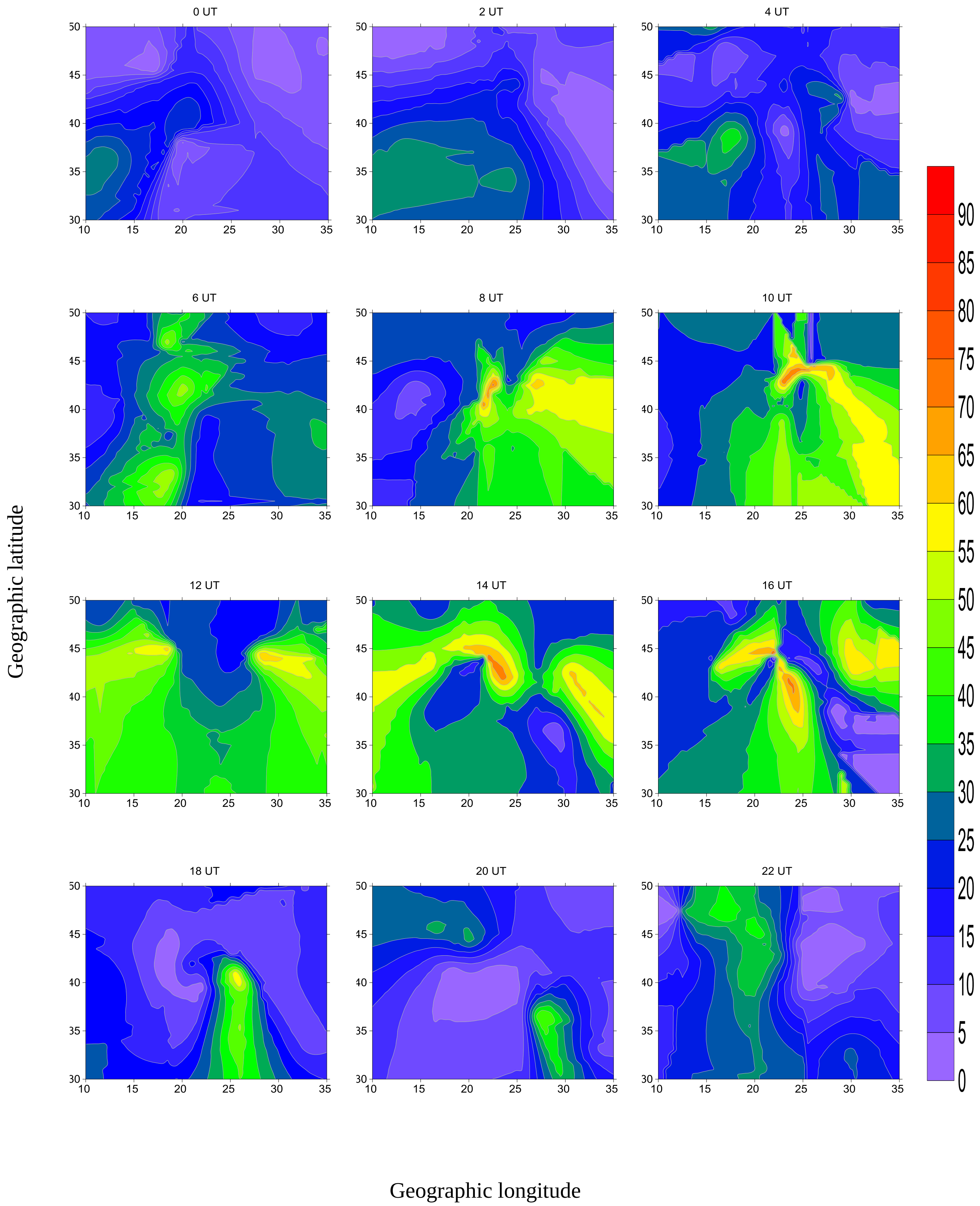

Figure (10). VTEC maps for SOFI station of Day 96 (2015).

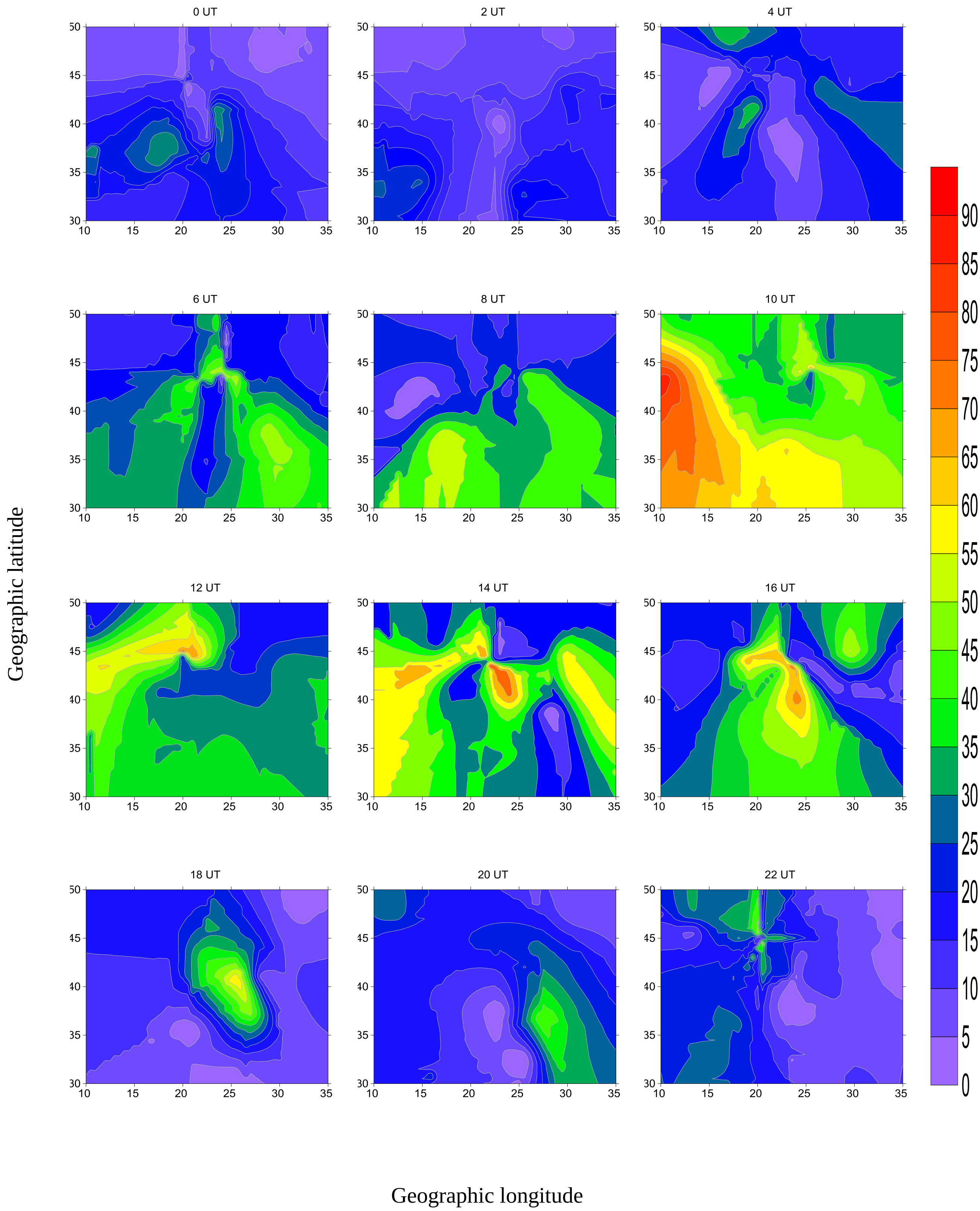

Figure (11). VTEC maps for SOFI station of Day 105 (2015).

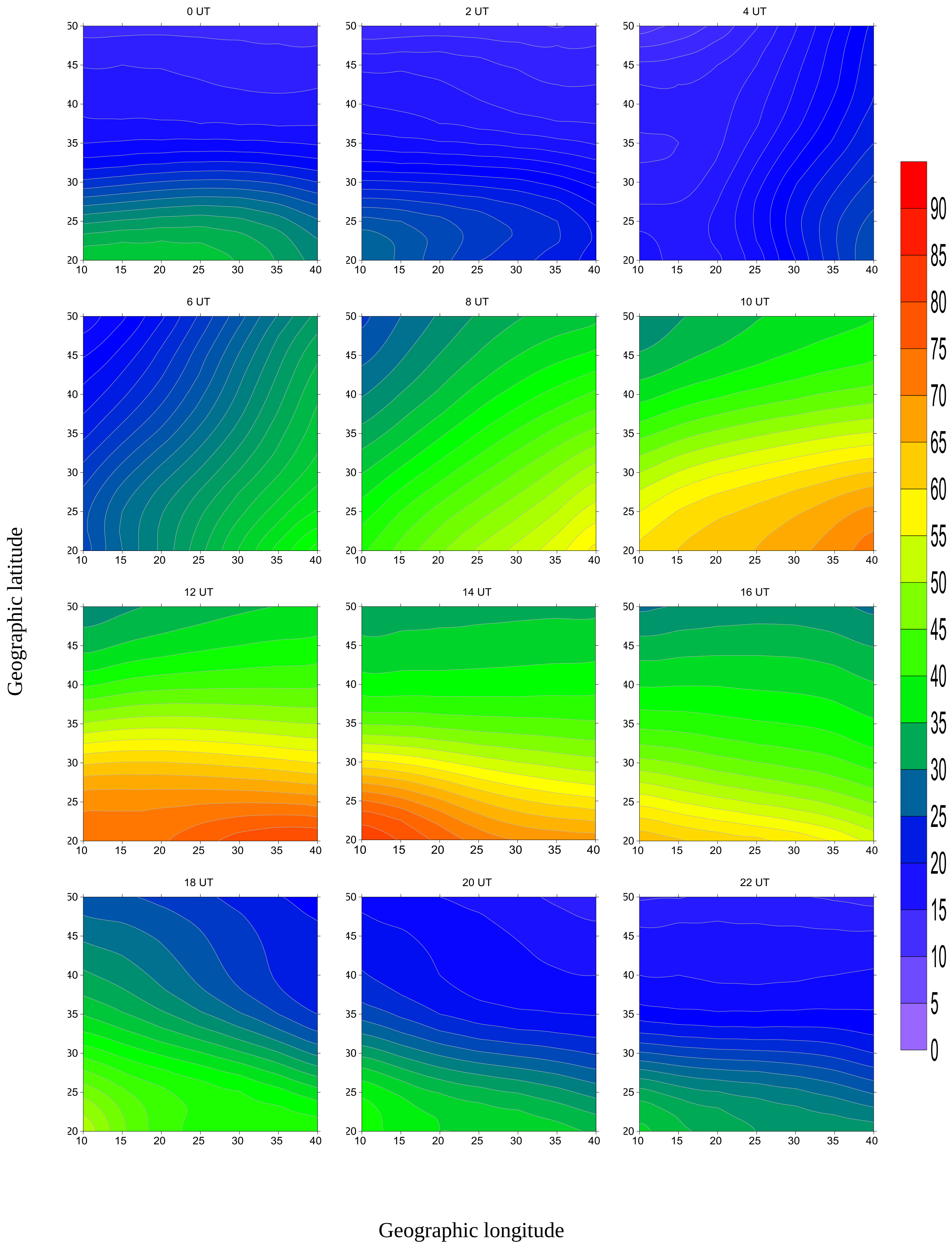

Figure (12) TEC maps from GIM, Day 96-2015.

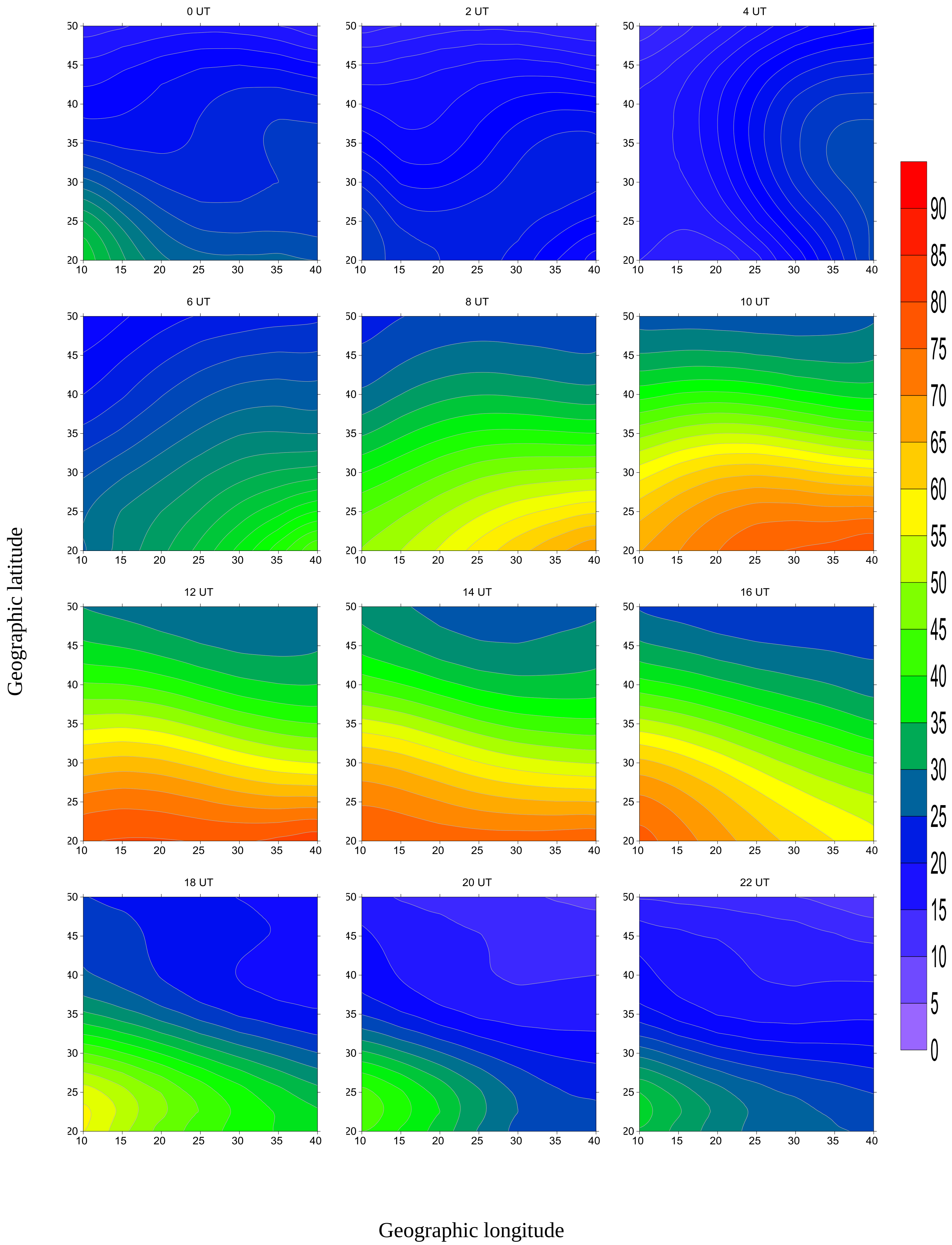

Figure (13) TEC maps from GIM, Day 105-2015.

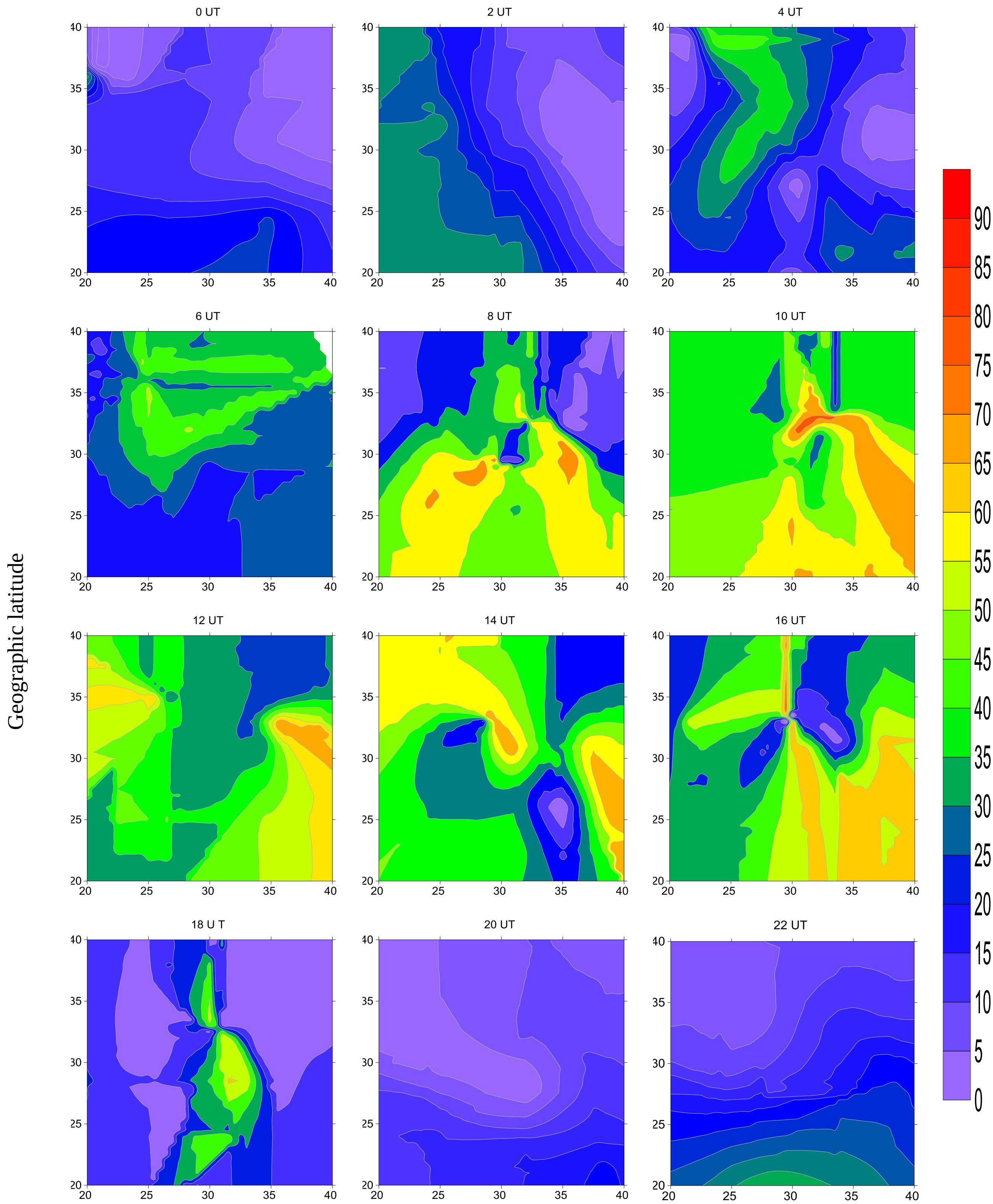

Geographic longitude

Figure (14) VTEC maps for HELW station of Day 96-2015.

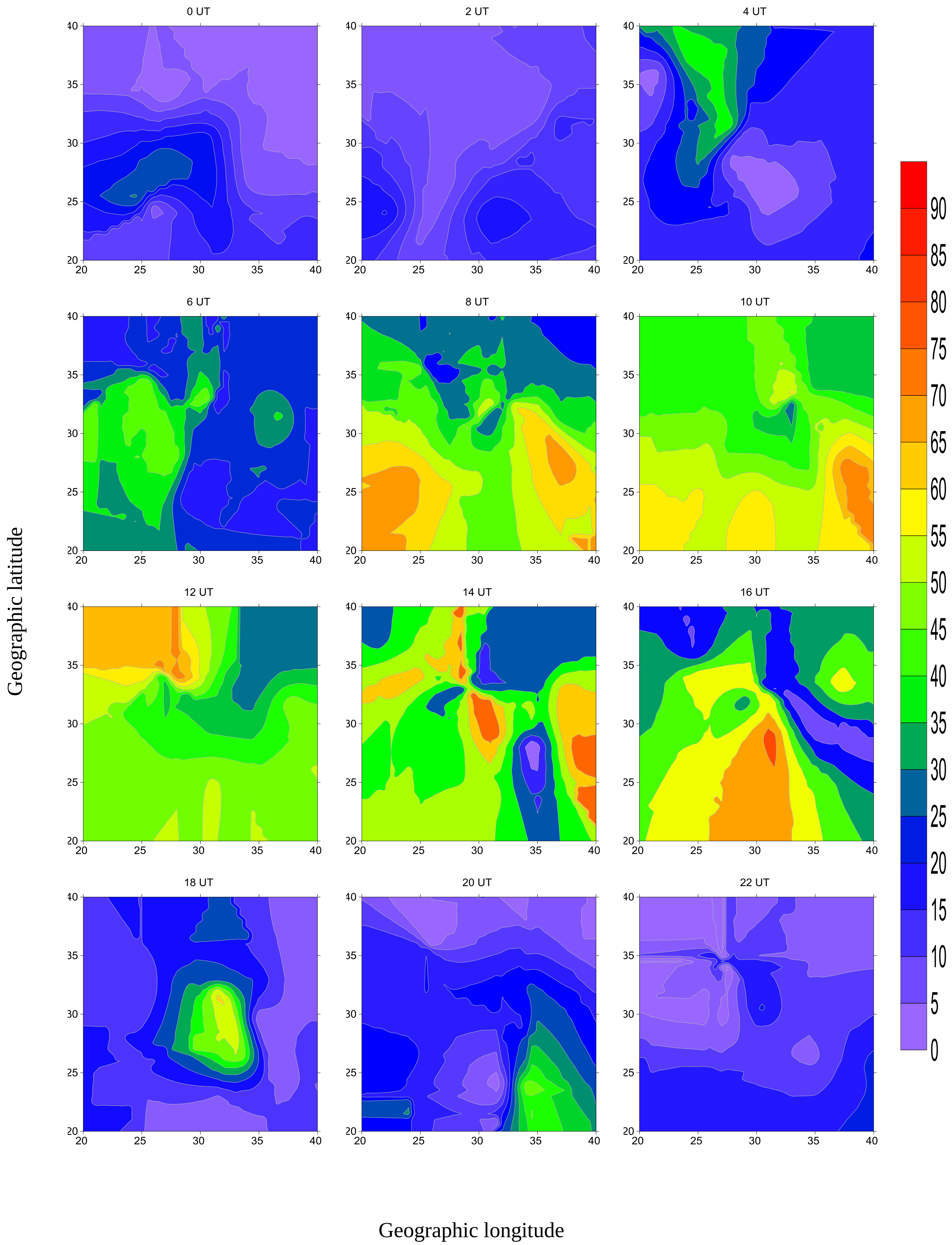

Figure (15) VTEC maps for HELW station of Day 105-2015.

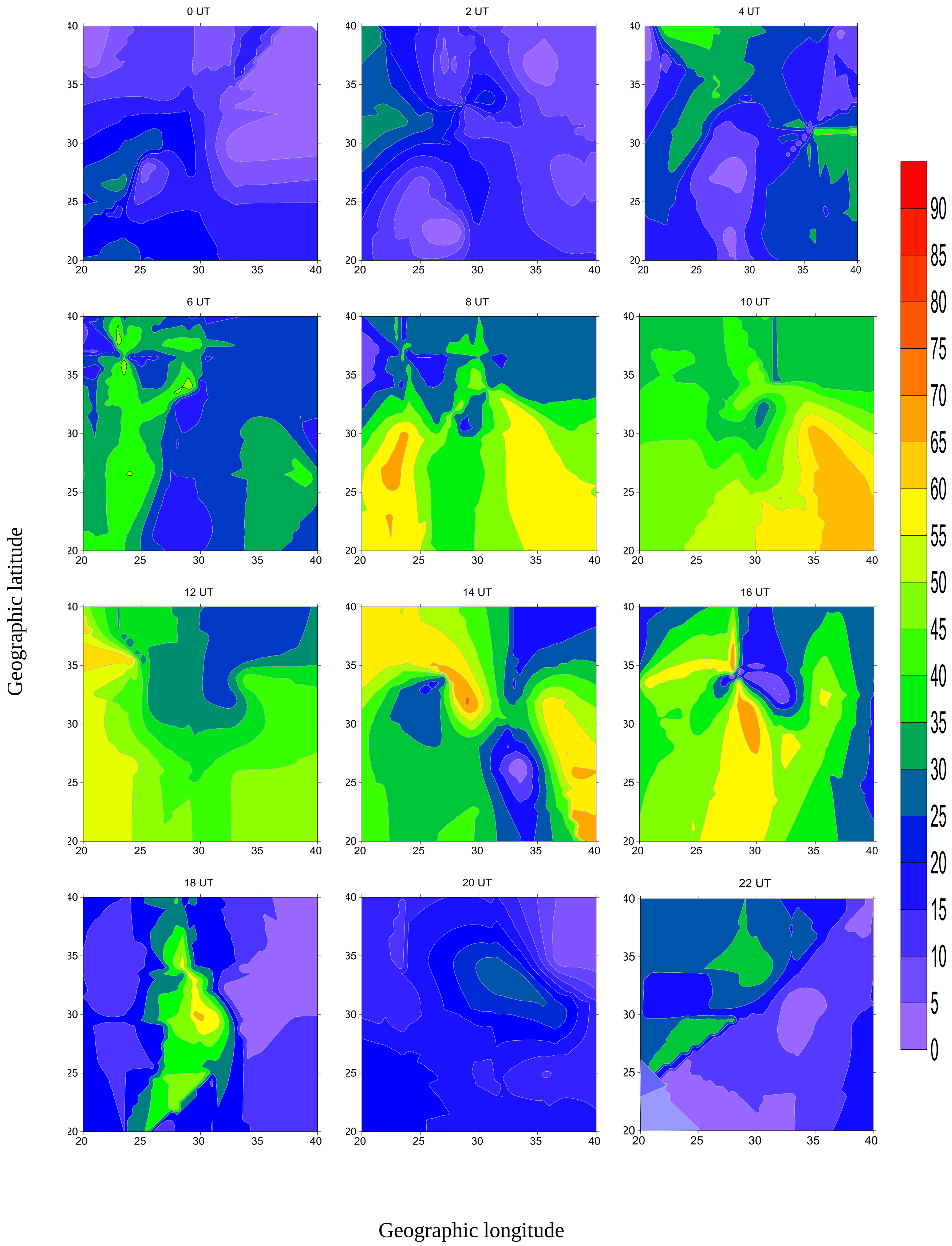

Figure (16) VTEC maps for SAID station of Day 96-2015.

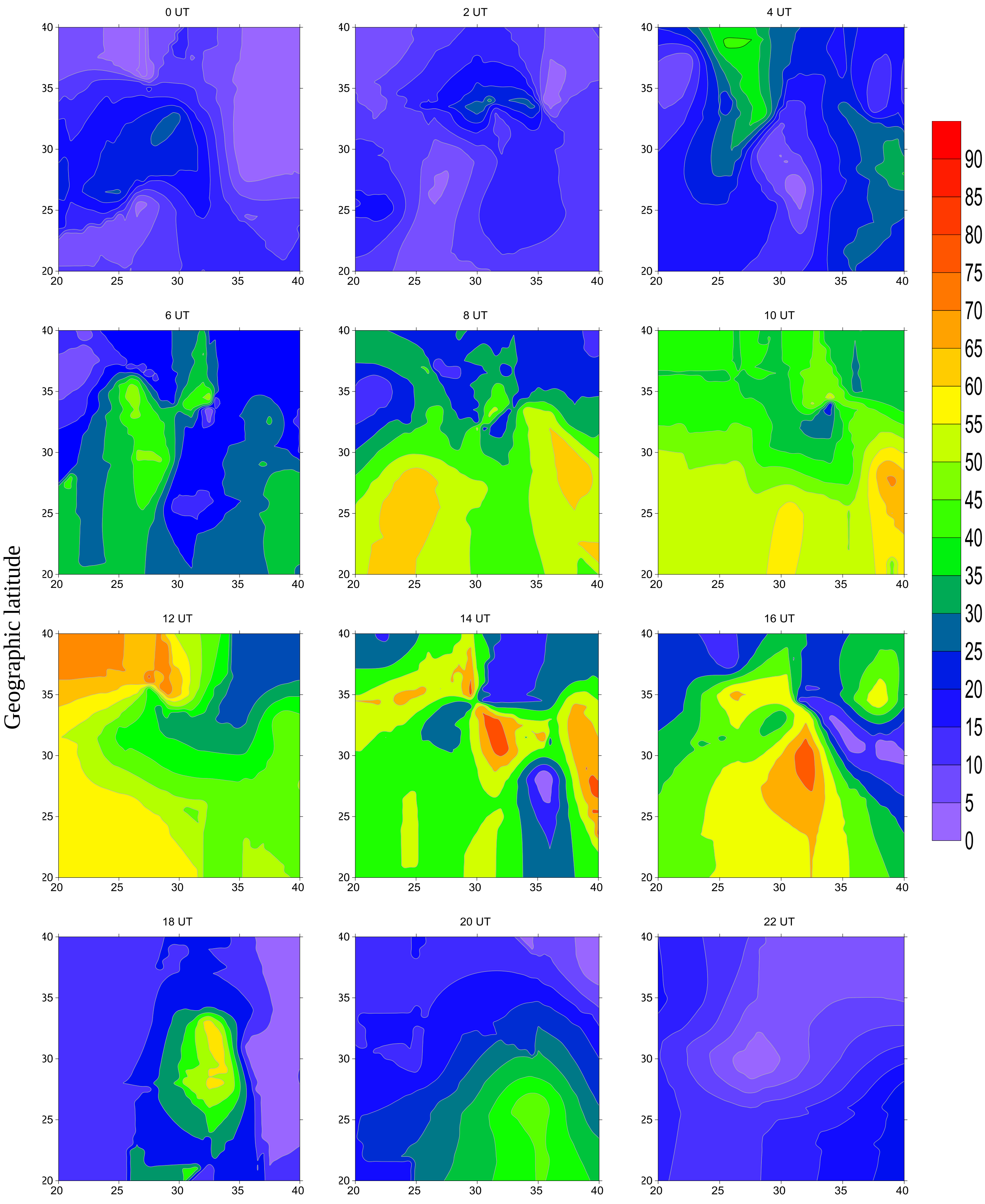

Geographic longitude

Figure (17) VTEC maps for SAID station of Day 105-2015.

As it is depicted in figures (6-7, 10-11, 14-15 and 16-17), ZDPID gives a much more detailed picture of the local ionosphere map. The IGS GIMs are a combination of TEC derivation from GPS observations, as well as different TEC modeling techniques.

This also explains why the TEC derived from GIMs is very smooth over the region. In contrast to the GIMs explains the global nature of GIMs maps. But ZDPID gives real perception of the local ionosphere map. Moreover, the Inverse Problem to retrieve such VTEC maps from the Slant TEC (STEC) measurements is not straightforward. This is because these measurements do not directly provide the STEC (the carrier phases are affected by the ambiguity term, and the pseudoranges by the interfrequency code bias, see for instance Hernández-Pajares et al., 2008. This is due to the current lack of GNSS ground receivers, especially over the Oceans and in the Southern Hemisphere, among other regions.

The obtained mean TEC values every 2 hours of the two IGS stations, using the ZDPID are shown in figure (18) for day 96-2015. As it is shown in the figure, The TEC difference between ZDPID over METS station and GIM varies from-2.6to 3.5 TECU and varies from -0.68 to 3.53 TECU for SOFI station. The TEC difference between GIM and ZDPID over SAID station is from - 2.1 to 4.1 TECU and varies from -1.7 to 3.1 TECU for HELW station.

IGS Analysis centers (ACs)often use TEC representation algorithms, which result in a model resolution comparable with the whole area of the region under investigation (Schaer, 1999). Wielgosz et al., (2003b) presented an example ionosphere maps for the Ohio CORS compared to the global GIMs. The GIMs general TEC level is higher by about 3-5 TECU, as compared to the maps generated using the Kriging and Multiquadric methods.

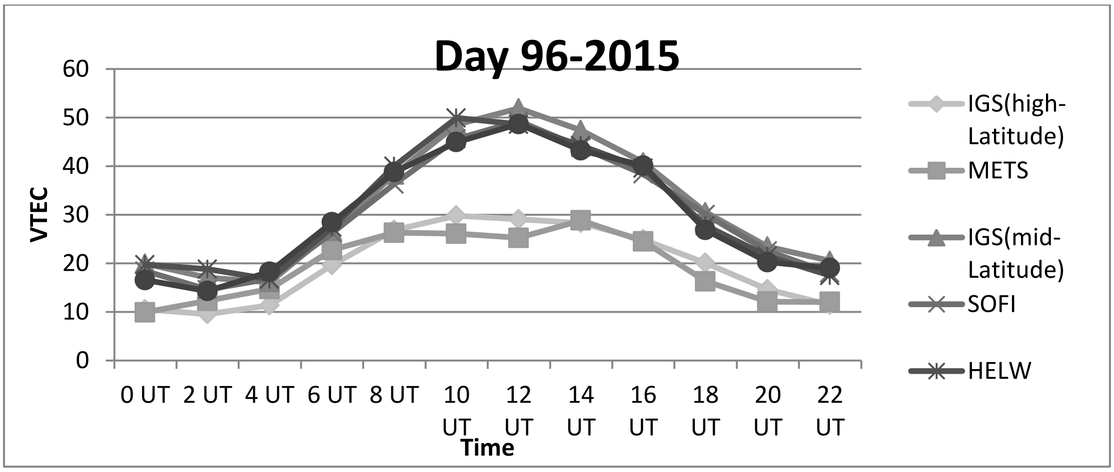

Figure (18) Mean TEC results every 2 hours of the Delta stations and IGS GIMs for day 96-2015.

Regional ionosphere maps have been generated for both quiet and stormy days by using Bernese 5.0 PPP model by Salih Alcay et al. (2012). They found that the biggest difference between single stations based regional model and GIMs are about 6 TEC in quiet day. However differences can reach 10 TECU for the some.

time periods of stormy day. Results of our model confirmed that, for regional VTEC maps are generally compatible with GIMs particularly.

Figure (19) shows the mean TEC values every 2 hours of stormy day (105-2015). The difference rang between METS station and IGS GIM is -2.6to 3.5 TECU and this rang is -3.37 to 4.7 TECU for SOFI station. The difference rang between IGS GIM and SAID station is from - 1.2 to 4.7 TECU, from -1.2 to 4.9 TECU for HELW station. The results of the proposed algorithm are able to estimate TEC efficiently. It is clear in figures (18&19) that the mean TEC values in stormy day are bigger than in quite day.

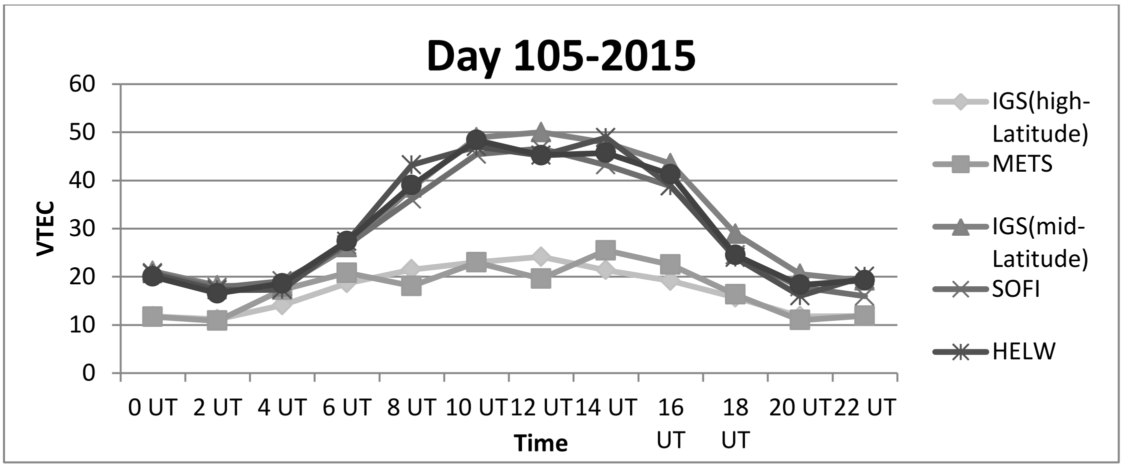

Figure (19) Mean TEC results every 2 hours of the Delta stations and IGS GIMs for day 105-2015.

4. Conclusions

The ionospheric behavior are needed to be characterized for satellite based positioning by TEC maps. Many studies have been performed for TEC mapping. In order to investigate the compatibility of these maps with GIMs, which is generally used as a reference, two stations have been selected from mid-latitude and high-latitude regions. Regional vertical TEC maps have been obtained by using MATLAB code, Zero-differenced phase Ionospheric Delay (ZDPID) for both quiet and stormy days. In order to determine the geographical location of the regional maps, coverage circle concept has been taken into consideration.

Results confirmed that, for both mid-latitude and high-latitude stations, regional vertical TEC maps are generally compatible with GIMs particularly when the quiet day is considered.

The computed GIMs of IGS suffered from the lack of stations at some areas (e.g., over the oceans), e.g. lack of data over the equatorial, North Africa, Atlantic and in-part over equatorial and southern Pacific. This shortage of data, hamper the detection of the equatorial anomalies. To overcome this shortage over Egypt and similar regions, and to improve the temporal and spatial resolution of regional VTEC maps in Egypt.

The mean TEC value the mean TEC values in stormy day are bigger than in quite day. ZDPID gives a much more detailed picture and real perception of the local ionosphere map from single point. On the other hand, results of the verification process are clearly shown that the developed algorithm can be successfully used for generating regional ionosphere maps.

5. References

Dahira jsunehra(2013), Validation of GPS receiver instrumental bias results for precise navigation. Indian Journal of Radio& space Physics, Vol. 42June 2013.pp.175-181.

Guochang Xu (2004), GPS Theory, Algorithms and Applications, Library of Congress Control Number: 2007929855. ISBN second edition 978-3-540-72714-9 Springer Berlin Heidelberg New York.

Hargreaves, J.(1992), The Solar-Terrestrial Environment: An Introduction to Geospace, Cambridge Atmospheric and Space Science Series, Cambridge University Press, Cambridge, 1992.

Hernández-Pajares M, Juan JM, Sanz J (2008), GPS data processing: code and phase Algorithms,TechniquesandRecipes.http://www.gage.es/TEACHING_MATERIAL/GPS_BOOK/ENGLISH/PDGPS/BOOK_PDGPS_gAGE_NAV_08.pdf, Barcelona, issue 2E, February

Jakowski,N., E. Sardon, E. Engler, A. Jungstand, and D. Klln (1996),Relationships Between GPS Signal Propagation Errors and EISCAT Observations, Annales Geophysicae, Vol. 14, pp. 1429-1436.

Liu, Z. and Gao, Y. (2004), Ionospheric TEC Predictions Over a Local Area GPS Reference Network. *GPS Solutions*, vol. 8, no. 1, pp. 23-29.

Melbourne W.G. (1985), The case for ranging in GPS based geodetic systems, Proceedings of the 1st international symposium on precise positioning with the global positioning system, Rockville, Maryland, pp 373–386.

Misra P. and Enge P., (2001), "Global Positioning System Signals, Measurements and Performance", Ganga Jamuna Press, MA, USA.

Misra P. and Enge P., (2006), Global Positioning System: Signals, Measurements, and Performance, 2nd edn. IGanga-Jamuna Press, Massachusetts.

Nohutcu, M., Karslioglu, M.O., Schmidt, M. (2010), B-Spline Modeling of VTEC Over Turkey Using GPS Observations, Journal of Atmospheric and Solar-Terrestrial Physics.72 pp.617-624.Systems Theory and Its Applications—III.

Rocken, C., M. Johnson, and J. Braun (2000), Improving GPS surveying with modeled ionospheric corrections", Geophys. Res. Lett., 27, 3821–3824.

Salih Alcay, CemalOzer Yigit, CevatInal (2012),GPS Based Ionosphere Mapping Using PPP Method, FIG Working Week 2012Knowing to manage the territory, protect the environment, evaluate the cultural heritage Rome, Italy, 6-10 May 2012.TS09B - Precise Point Positioning, 5618 1/11.

Sardon, E., N. Jakowski, and N. Zarraoa (1995),Permanent Monitoring of TEC Using GPS Data: Scientific and Practical Aspects., EOS Transactions of the American Geophysical Union, Vol. 76, No. 17, Supplement, p. 87 (abstract).

Schaer, S. (1999),Mapping and Predicting the Earth's Ionosphere Using the Global Positioning System, PhD dissertation, Astronomical Institute, University of Berne, Switzerland, pp. 205.

Sedeek A. A., Doma M. I., Rabah M. and Hamama M. A. (2017), Determination of Zero Difference GPS Differential Code Biases for Satellites and Prominent Receiver Types, Arabian journal of geosciences, vol. 10, January 2017.

Stanislawska, I., Juchnikowski, G., Hanbaba, R., Rothkaehl, H.,G. Sole, and Z. Zbyszynski(2000), COST 251 Recommended Instantaneous Mapping Model of Ionospheric Characteristics – PLES, Phys. Chem. Earth (C), vol. 25, no. 4, pp. 291-294.

Sunehra D., (2013), "Validation of GPS Receiver Instrumental Bias Results", Indian Journal of Radio & Space Physics, Vol. 42, June 2013, PP 175-181.

Wielgosz P., L.W. Baran, I.I. Shagimuratov and M.V. Aleshnikova (2003a),Latitudinal variations of TEC over Europe obtained from GPS observation, accepted by Annales Geophysicae.

Wielgosz, P., Grejner- Brzezinka, D. and Kashani, I. (2003b),Regional Ionosphere Mapping with Kriking and Multiquadric Methods, Journal of Global Positioning Systems, vol. 2, no. 1, pp 48-5.